Limitations of Metric Loss for the Estimation of Joint Translation and Rotation

Philippe Pérez de San Roman[1,2,3], Pascal Desbarats[1,2], Jean-Philippe Domenger[1,2] and Axel Buendia[3,4,5]

[1] *Université de Bordeaux, Bordeaux, France*

[2] *LaBRI, Talence, France*

[3] *ITECA, Angoulłme/Paris France*

[4] *SpirOps, Paris, France*

[5] *CNAM-CEDRIC, Paris, France*

https://www.u-bordeaux.com/, http://www.labri.fr/, http://iteca.eu/, http://www.spirops.com/, https://cedric.cnam.fr/

Keywords: Object Localization, Deep Learning, Metric Loss.

Abstract: Localizing objects is a key challenge for robotics, augmented reality and mixed reality applications. Images taken in the real world feature many objects with challenging factors such as occlusions, motion blur and changing lights. In manufacturing industry scenes, a large majority of objects are poorly textured or highly reflective. Moreover, they often present symmetries which makes the localization task even more complicated. PoseNet is a deep neural network based on GoogleNet that predicts camera poses in indoor room and outdoor streets. We propose to evaluate this method for the problem of industrial object pose estimation by training the network on the T-LESS dataset. We demonstrate with our experiments that PoseNet is able to predict translation and rotation separately with high accuracy. However, our experiments also prove that it is not able to learn translation and rotation jointly. Indeed, one of the two modalities is either not learned by the network, or forgotten during training when the other is being learned. This justifies the fact that future works will require other formulation of the loss as well as other architectures in order to solve the pose estimation general problem.

1 INTRODUCTION

Over the past decades, the growing interest for Deep Convolutional Neural Networks for image and object recognition (Le Cun et al., 1990; Krizhevsky et al., 2012; Szegedy et al., 2015; Simonyan and Zisserman, 2014) has seen more ambitious works emerged for image segmentation (Ronneberger et al., 2015) and object localization (Kendall et al., 2015; Rad and Lepetit, 2017; Do et al., 2018; Li et al., 2018; Xiang et al., 2017). Object localization is a key component for augmented reality applications where information, visual effects or data are added to real world objects. This allows the user to be better informed about his environment, most often by wearing an augmented reality headset (Microsoft Hololens®, 2017). Augmented reality is applied in video-game industry and shopping Industry (IKEA, 2017). It is also useful in the medical domain (Collins et al., 2014) and in manufacturing industry (Didier et al., 2005).

Typical augmented reality headsets have a transparent screen inserting visuals on the foreground of the user's field of view. As for now, headsets such as the (Microsoft Hololens®, 2017) provide limited data about user environment (RGB video, surface mesh of nearby objects). They have also limited memory and computational power. It is thus difficult to align the created visuals on the real world objects, especially if high precision is required as it is the case in many industrial or medical applications. To enable the deployment of such technologies in applicative fields with high robustness constraints, the precision of object localization as to be drastically increased. Moreover, challenging objects (namely: objects without texture, objects with metallic materials and symmetric objects) have to be correctly handled.

In this paper we are interested in localizing industrial objects with high precision for augmented reality

Roman, P., Desbarats, P., Domenger, J. and Buendia, A.
Limitations of Metric Loss for the Estimation of Joint Translation and Rotation.
DOI: 10.5220/0007525005900597
In *Proceedings of the 14th International Joint Conference on Computer Vision, Imaging and Computer Graphics Theory and Applications (VISIGRAPP 2019)*, pages 590-597
ISBN: 978-989-758-354-4

applications in the manufacturing industry. We aim to deploy such solutions on augmented reality headsets. To that extent, we selected PoseNet (Kendall et al., 2015) as the backbone architecture and trained it on the T-LESS dataset(Hodaň et al., 2017) as it features 30 industrial objects and it consists in very detailed training data which perfectly suits our needs in order to train a CNN to localize objects. In this particular setup, we will focus on the influence of the two parameters of PoseNet in order to find the best weighting to ensure optimal pose estimation. These two parameters weigh the importance of the translation estimation and rotation estimation respectively. Therefore, we provide a thorough evaluation of their impact on the training using PoseNet when applied to the T-LESS dataset. Our experiments will show that the network is not able to correctly learn both modalities together as one modality always overtakes the other.

Overview of the Paper. In the next part we present the state of the art in object localization and available datasets. Then we detail the experimental protocol used measure if translation and rotation can be learned jointly, starting with the dataset: T-LESS (Hodaň et al., 2017), the network proposed by A. Kendall and al: PoseNet (Kendall et al., 2015), the loss function optimized during training, and the accuracy measurement performed. Following section describes the results we obtained that prove that translation and rotation can be learned separately but not together. Finally we interpret these results with regards to the task of augmented reality for manufacturing industry, and we propose possible solutions that we intent to explore in the near future.

2 STATE OF THE ART

The task of object / camera pose estimation has been widely covered in previous works. Structure-From-Motion algorithms (Häming and Peters, 2010) can retrieve the position and orientation of a camera given a set of images using descriptors such as SIFT (Lowe, 1999) or SURF (Bay et al., 2006) and RANSAC regression. More recently, deep-learning methods have overpassed manual descriptors as they are now able to learn more specific features for each application, providing better results on most challenges. Modern CNNs such as PoseNet (Kendall et al., 2015) can be used to directly predict the pose of an object. These methods were extended to predict the pose of multiple parts (Crivellaro et al., 2015a) in order to increase the robustness of the network towards occlusions. Other approaches aim at regressing the position of the 8 corners of the bounding-box of the object in the image plane to recover 3D coordinates using PnP algorithms (Rad and Lepetit, 2017). Methods with multiple regression branches have also been proposed in (Do et al., 2018; Xiang et al., 2017). Finally, methods with iterative refinement on the estimated pose have recently appear (Li et al., 2018) in order to increase overall precision. Pose detection applied to augmented reality requires real-time performances as well as low memory consumption. Thus, multi-part / multi-branches approaches are oversized for our application scenario. Moreover, object of attention is usually located in the center of the image, on the foreground. Therefore, the robustness towards occlusion is not relevant here. Therfore, we chose the PoseNet architecture as the backbone of the presented work.

The Extented ACCV (Crivellaro et al., 2015b) dataset is designed for training methods on 3D models. However, it has shown limitations in its usage as each image has to be rendered to generate training dataset. Datasets for autonomous driving such as (Geiger et al., 2012) have been widely used because of their high quality. However, such datasets focus on outdoor scenarios at metric precision. On the other hand, the T-LESS (Hodaň et al., 2017) dataset focuses on industrial objects with centimetric precision in the groundtruth. Moreover, it depicts objects without textures that are typically found in industrial environment (electrical parts). Thus, the T-LESS dataset perfectly fits our requirements in terms of precision and object diversity.

3 EXPERIMENTAL SETUP

We aim to find the 3D position of industrial objects in RGB video for augmented reality applications using deep learning techniques. The goal of the experiments reported in this paper are to show that the Euclidean loss does not allow training the (Kendall et al., 2015) network to predict accurate pose estimation of translation and rotation on the selected dataset. In this section we first present in depth the dataset we use: T-LESS(Hodaň et al., 2017), then we describe the architecture of the network proposed in (Kendall et al., 2015), followed by the loss function used to train the network, and finally the accuracy metrics that are applied in our experiments.

T-LESS Dataset. The T-LESS dataset (Hodaň et al., 2017) features objects with no discriminating colors, metallic parts, intern similarities and symmetries. Therefore, it is a very challenging dataset to work on. The training set only depicts a single object on a black background in each image. On the opposite, the testing set consists in many objects on various backgrounds for each image. As we are focused on selecting the optimal α and β parameters of the loss function Equation (1), the network is trained on a split of the training set and accuracy is computed on the rest of the training set.

PoseNet Architecture. PoseNet (Kendall et al., 2015) is among the first networks that successfully tackled the problem of camera re-localization. It is a 20 modules deep convolutional neural network. The fact that it based on GoogleNet (Szegedy et al., 2015) gives it interesting properties: low memory usage (only 4 million parameters), fast evaluation and the ability to work with features at different scales. We apply the same weight to the auxiliary classifier as in (Szegedy et al., 2015) $(0.3, 0.3, 1)$ For details about the complete architecture of the network we invite the interested reader to read the work of (Szegedy et al., 2015) and (Kendall et al., 2015) but we also provided a graphical representation of the architecture in the Figures 1,2 in appendices.

Joint Euclidean Loss. The network is trained to optimize the following joint euclidean loss function:

$$L(\widehat{t_i}, t_i, \widehat{q_i}, q_i) = \alpha \times \left\| \widehat{t_i} - t_i \right\|_2 + \beta \times \left\| \widehat{q_i} - \frac{q_i}{\|q_i\|_2} \right\|_2 \tag{1}$$

Where $i \in [0, b]$ is the index of the example in a batch of size b, $\widehat{t_i}$ is the predicted translation (3D vector), $\widehat{q_i}$ the predicted rotation, t_i is the translation label (3D vector) and q_i is the rotation label.

The weighting factors α and β are used to respectively weight the translation error, and the rotation error. The quaternion error if both $\widehat{q}$ and q are unit length, is bounded in $[0, 2]$ although in the first step where the network weight are randomly initialized, this loss value could actually be higher. The same is true for the translation error but it is mostly influenced by the scale and the unit in which data are presented to the network. T-LESS data are provided in millimeters, the maximum distance is $700mm$. This means that the error could be of at least of $3880mm \times b^1$ and more for the 3 classification branches used during training (where b is the batch size).

Such high values for a loss are challenging because they can lead to numerical error when computing the gradient. Thus the α and β parameters have tremendous impact on the training stability and as we will see on accuracy of the network at prediction time.

[1] $loss = \sqrt{(2 \times (700mm + 700mm))^2} = 2800mm$, and $lossglobal = loss + 0.6 \times loss = 3880mm$

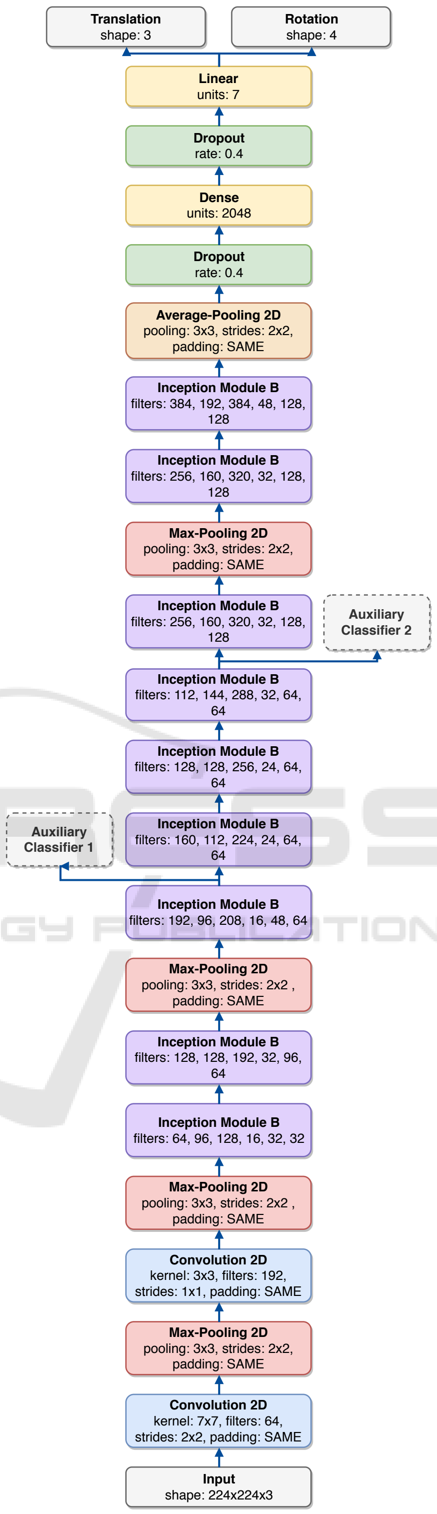

Translation shape: 3
Rotation shape: 4
Linear units: 7
Dropout rate: 0.4
Dense units: 2048
Dropout rate: 0.4
Average-Pooling 2D pooling: 3x3, strides: 2x2, padding: SAME
Inception Module B filters: 384, 192, 384, 48, 128, 128
Inception Module B filters: 256, 160, 320, 32, 128, 128
Max-Pooling 2D pooling: 3x3, strides: 2x2, padding: SAME
Inception Module B filters: 256, 160, 320, 32, 128, 128
Auxiliary Classifier 2
Inception Module B filters: 112, 144, 288, 32, 64, 64
Inception Module B filters: 128, 128, 256, 24, 64, 64
Auxiliary Classifier 1
Inception Module B filters: 160, 112, 224, 24, 64, 64
Inception Module B filters: 192, 96, 208, 16, 48, 64
Max-Pooling 2D pooling: 3x3, strides: 2x2 , padding: SAME
Inception Module B filters: 128, 128, 192, 32, 96, 64
Inception Module B filters: 64, 96, 128, 16, 32, 32
Max-Pooling 2D pooling: 3x3, strides: 2x2 , padding: SAME
Convolution 2D kernel: 3x3, filters: 192, strides: 1x1, padding: SAME
Max-Pooling 2D pooling: 3x3, strides: 2x2, padding: SAME
Convolution 2D kernel: 7x7, filters: 64, strides: 2x2, padding: SAME
Input shape: 224x224x3

Figure 1: Backbone architecture of PoseNet(Kendall et al., 2015) with parameters of each layers. The two auxiliary classifiers detailed in figure 2 and the dropout layers are only used during training.

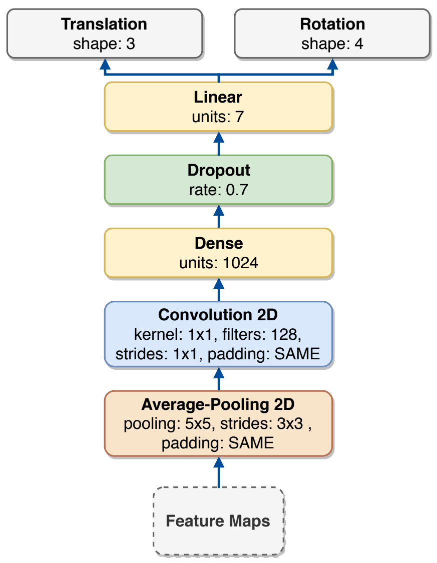

Figure 2: Architecture of the two auxiliary classifiers of PoseNet(Kendall et al., 2015) with parameters of each layers used only during training.

The intuition here is that scaling α down will prevent the translation from dominating the loss, allowing rotation to train as well and ensuring computational integrity. β can also be scaled up to better focus the training on rotation.

Euclidean Accuracy. We advocate that the accuracy is directly influenced by the ability of the network to learn jointly translation and rotation which is controlled by the α and β parameters in Equation (1).

The translation accuracy can be measured by the euclidean distance to τ:

$$Acc_{cm}(\widehat{t},t,\tau)=\sum_{i=0}^{N}\begin{cases}\frac{1}{N} & \text{if } \left|\left|\widehat{t}-t\right|\right|_2 \leq \tau \\ 0 & \text{otherwise}\end{cases} \quad (2)$$

A predicted translation $\widehat{t}$ (in cm) is considered correct if the euclidean distance between the prediction $\widehat{t}$ (in cm) and the label t (in cm) is less than a given threshold τ (in cm).

One way to compute the rotational accuracy is using the angle at τ:

$$Acc_o(\widehat{q},q,\tau) = \sum_{i=0}^{N}\begin{cases}\frac{1}{N} & \text{if } angle(\widehat{q},q) \leq \frac{\tau\times\pi}{180} \\ 0 & \text{otherwise}\end{cases} \quad (3)$$

$$angle(\widehat{q},q) = \arccos(2\times\langle\frac{\widehat{q}}{||\widehat{q}||_2},\frac{q}{||q||_2}\rangle^2-1) \quad (4)$$

A predicted rotation $\widehat{q}$ (quaternion) is considered correct if the angle (in degree) between the prediction $\widehat{q}$ (quaternion) and the label q (quaternion) is less than a given threshold τ (in degree). Note that $angle(\widehat{q},q)$ gives an angle in radians thus we convert the threshold τ to radians in the above equation.

Complete Setup. We train the PoseNet network(Kendall et al., 2015) to regress translation (3D vector) and rotation (4D quaternion) by optimizing an euclidean loss as defined in Equation (1) like in (Kendall et al., 2015) on data from the T-LESS dataset (Hodaň et al., 2017). The images of a subset of the training set of the dataset are re-sized to a fixed size of 224x224 (RGB). We do not take crops nor apply any data augmentation. The learning rate is set to $\gamma = 0.0001$ for all training runs. We do this training several time with various values of α and β to show the effect of these two parameters on the training in terms of convergence speed, stability, and on the accuracy for both translation and rotation (measured on the remaining examples of training set).

4 RESULTS

Choosing the right value for α and β is a very complicated task. In this section we detail all the training run and provide interpretation of the results. We first produced baseline results for translation and rotation where one of the two weight is set to 0 only allowing one of the two to train. Then following our intuition we fixed β to 1 and attempted to scaled down α. And finally we fixed α and scaled β up in an attempt to better learn rotation.

Baseline Results. We first set the parameters to $\alpha = 0.01, \beta = 0$ (only optimizing translation). Results are presented in Figure 3 **(a)**. In order to visualize the results we rendered the objects at ground truth position and ground truth rotation in green, and overlay a render of the object at predicted position and at ground truth rotation in transparent red. As expected the networked learned to predict accurate translation but not rotation. The accuracy for the translation is equal to 20% for $\tau = 5cm$ and is equal to 100% for $\tau \geq 20cm$.

Then we set the parameters to $\alpha = 0, \beta = 1$ (only optimizing rotation). Figure 3 **(b)** features objects rendered at the ground truth position and ground truth rotation in green and objects rendered at the ground truth position but predicted rotation in red. This time the network is very accurate on rotation and inaccurate on translation. With $Accu_o(\widehat{q},q,5^o) = 26\%$ and for $\tau \geq 20^o$ then $Accu_o(\widehat{q},q,\tau) \approx 100\%$. Translation accuracy is close to 0 for any values of $\tau \leq 65cm$. We recall that object are at most $70cm$ away from the

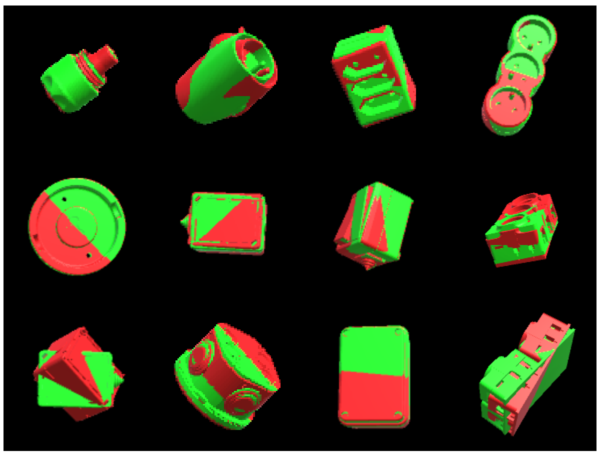
(a) $\alpha = 0, \beta = 1$

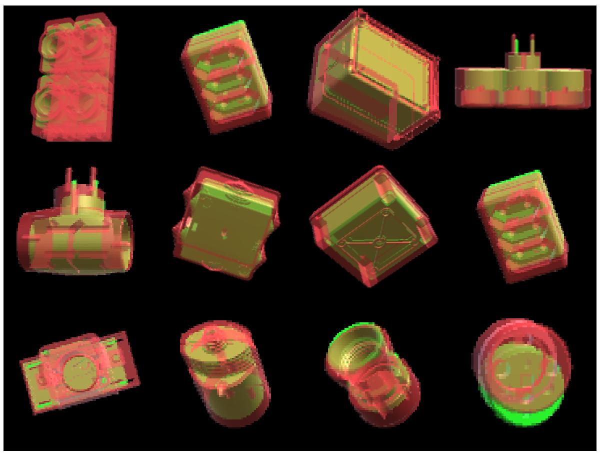
(b) $\alpha = 0.01, \beta = 0$

Figure 3: **(a)** Results for a network trained to only optimize rotation ($\alpha = 0, \beta = 1$). Green: objects at the ground truth t and q, red: objects at the ground truth t but predicted $\widehat{q}$. **(b)** Results for a network trained to only optimize translation ($\alpha = 0.01, \beta = 0$). Green: object at the ground truth t and q, red: objects at the ground truth q but predicted $\widehat{t}$.

camera in T-LESS so for any value of $\tau > 65cm$ the accuracy will always be close to 100%.

Together these two classifiers provide a good solution to the problem of object localization in terms of accuracy. But we would like to combine these two results in one network following the work of (Kendall et al., 2015) to save memory and computational time as well as providing a unified solution to the problem.

Down-scaling Translation. In order to prevent the translation loss from taking to large values with respect to the rotation loss, and also to ensure computational integrity of the gradient we fixed the β parameter to 1 and started tuning the α parameter. Results on the loss (translation and rotation) can be found in Figure 4 **(a)** and results on the accuracy can be found in Figure 4 **(b)**.

Setting $\alpha \geq 0.0075$ does not allow rotation to be trained at all. This is equivalent to the baseline result where β is set to 0. Then if we set α to 0.005 or 0.006 we can see on Figure 4 **(b)** (second row) that rotation is learned but then as training progresses, it is forgotten to allow translation to be learned. This is also visible in Figure 4 **(a)**: as soon as translation loss decreases, rotation loss increases drastically. Even if the rotation loss then slowly decreases, it never returns to its previous minimum, and accuracy never increases again. Finally $\alpha \leq 0.001$ does not allow translation to be trained. Loss and accuracy are equivalent to the ones for $\alpha = 0$ (baseline result).

As we can see, setting only α is not enough. If we do no not decrease it, rotation will not be learned for sure. But decreasing it (without changing β) will only delay the translation from taking over. And if we decrease it too much we quickly fall back to the case where it is equal to 0.

Up-scaling Rotation. In the previous experiment we saw that $\alpha = 0.005$ is a key value where the loss "hesitates" between the translation and rotation. We also concluded that only tuning α is not enough to balance translation and rotation. In this set of experiments we wanted rotation to train just like it did before in the early stages of training, thus we set α to 0.005. But we also wanted it to not be forgotten by the network. To ensure this we increased β in values ranging from 1 to 3.Results are presented in Figure 5 **(a)** and **(b)**. We first set β to 0.5 and we saw as expected that this leads to rotation not being learned at all just like in our baseline result where β was set to 0. Then we increased β to 1.2 and 1.5. Results presented in Figure 5 **(b)** (second row) show that rotation is indeed learned longer, thus better. But we see the same phenomena as before: when translation is learned, rotation is forgotten. Thus we decided to further increase β and set it to 2 and 3. For these values translation accuracy did not increased, and the corresponding loss remains constantly high. This result is equivalent to the baseline result where $\alpha = 0$.

Once again this set of experiment shows that translation is favored to rotation during training. Translation and rotation can never be learned jointly with high accuracy for both. Rotation is either not learned at all, or forgotten. This is due to the fact that it is more profitable for the network to learn translation with respect to the implemented loss.

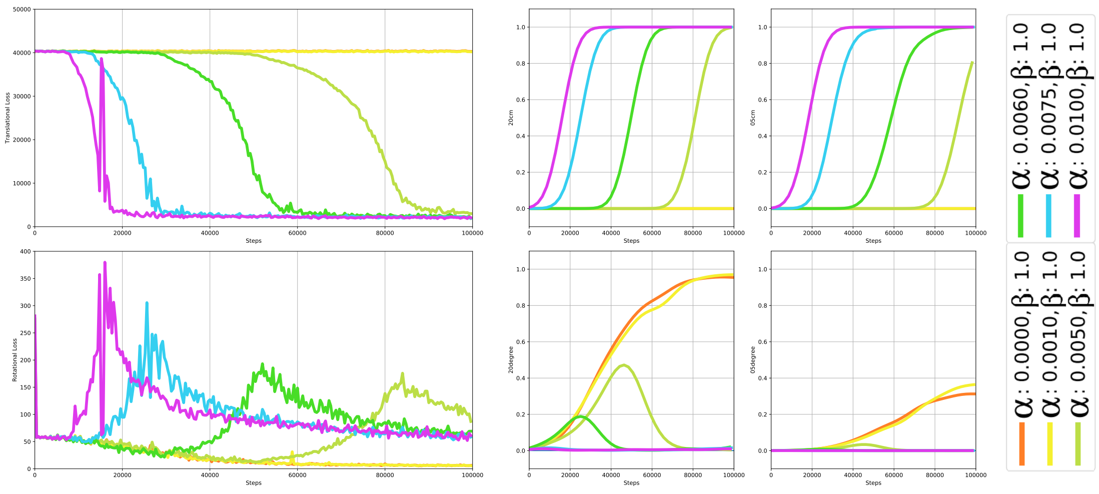

(a) Translation and rotation losses (b) Translation and rotation accuracies (c) Legend

Figure 4: First row: translation, second row: rotation. **(a)** Euclidean loss over training steps for different α values and $\beta = 1.0$ **(b)** Accuracy at $\tau = 20$ and $\tau = 5$ over training steps for different α values and $\beta = 1.0$.

5 CONCLUSIONS

Regressing both translation and rotation using a single regression branch is a very hard task for a network as it has to model different concepts (with different units) at the same level of abstraction. They are no values of the weighting parameters α and β that enable the network to learn jointly rotation and translation. If $\alpha > 0$, conflicts between translation and rotation occur, and translation overtakes rotation. The only effect of increasing β was to delay the overtaking of the translation.

The fact that we can see so clearly the PoseNet (Kendall et al., 2015) forgetting one of the two modality in favor of the other in the results proves that when used on the T-LESS dataset it is failing to learn translation and rotation jointly. This is mainly because the scale, and the range of viewpoints of the data is not the same as the original use case. PoseNet is meant for large scene where object are bigger and observed from further away and from less point of views. In our case the positional data in millimeter leads to large translation error that is not bounded. The rotational loss on the other hand is bounded by definition. Thus the translation always takes over in the training at some point.

Perspectives. To solve the problem of the euclidean loss not being able to learn jointly the translation and rotation, one could investigate the use of other losses that already exist, such as 3D geometrical loss for application that require absolute precision, or 2D geometrical loss computed in the image plane that are suitable for augmented reality applications (Brégier et al., 2016). These losses are very interesting because they can be modified to include symmetries. Other networks architectures that have separate regression branches for translation and rotation can also help training the two jointly (Do et al., 2018; Xiang et al., 2017). New types of network such as Capsules Network (Hinton et al., 2011; Sabour et al., 2017) that have vectorial activation values could better model translation and rotation that are vectorial data.

ACKNOWLEDGEMENTS

We would like to thank Pierre Biasutti for the long talk we had on the results presented in the paper and Arnaud Favareille, who both helped with the paper.

REFERENCES

Bay, H., Tuytelaars, T., and Van Gool, L. (2006). SURF: Speeded up robust features. In *In ECCV*, pages 404–417.

Brégier, R., Devernay, F., Leyrit, L., and Crowley, J. L. (2016). Defining the pose of any rigid object and an associated distance. *CoRR*, abs/1612.04631.

Collins, T., Pizarro, D., Bartoli, A., Canis, M., and Bourdel, N. (2014). Computer-assisted laparoscopic myomectomy by augmenting the uterus with pre-operative mri data. In *2014 IEEE International Symposium on Mixed and Augmented Reality (ISMAR)*, pages 243–248.

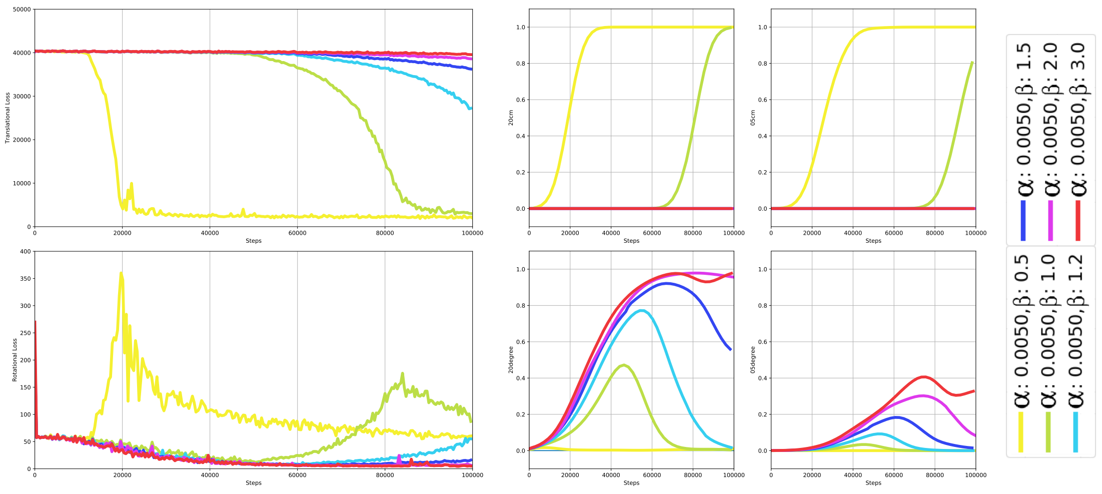

(a) Translation and rotation losses (b) Translation and rotation accuracies (c) Legend

Figure 5: First row: translation, second row: rotation. **(a)** Euclidean loss over training steps for $\alpha = 0.005$ and various values of β. **(b)** Accuracy at $\tau = 20$ and $\tau = 5$ over training steps for $\alpha = 0.005$ and various values of β.

Crivellaro, A., Rad, M., Verdie, Y., Yi, K., Fua, P., and Lepetit, V. (2015a). A novel representation of parts for accurate 3d object detection and tracking in monocular images. In *2015 IEEE International Conference on Computer Vision (ICCV)*, pages 4391–4399.

Crivellaro, A., Rad, M., Verdie, Y., Yi, K. M., Fua, P., and Lepetit, V. (2015b). A novel representation of parts for accurate 3d object detection and tracking in monocular images. In *Proceedings of the 2015 IEEE International Conference on Computer Vision (ICCV)*, ICCV '15, pages 4391–4399, Washington, DC, USA. IEEE Computer Society.

Didier, J.-Y., Roussel, D., Mallem, M., Otmane, S., Naudet, S., Pham, Q.-C., Bourgeois, S., Mégard, C., Leroux, C., and Hocquard, A. (2005). AMRA: Augmented reality assistance for train maintenance tasks. In *Workshop Industrial Augmented Reality, 4th ACM/IEEE International Symposium on Mixed and Augmented Reality (ISMAR 2005)*, page (Elect. Proc.), Vienna, Austria.

Do, T., Cai, M., Pham, T., and Reid, I. D. (2018). Deep-6DPose: Recovering 6D object pose from a single RGB image. *CoRR*, abs/1802.10367.

Geiger, A., Lenz, P., and Urtasun, R. (2012). Are we ready for autonomous driving? the KITTI vision benchmark suite. In *2012 IEEE Conference on Computer Vision and Pattern Recognition*, pages 3354–3361.

Häming, K. and Peters, G. (2010). The structure-from-motion reconstruction pipeline a survey with focus on short image sequences. *Kybernetika*, 5.

Hinton, G., Krizhevsky, A., and Wang, S. (2011). Transforming auto-encoders. In Honkela, T., Duch, W., Girolami, M., and Kaski, S., editors, *Artificial Neural Networks and Machine Learning – ICANN 2011*, pages 44–51. Springer Berlin Heidelberg.

Hodaň, T., Haluza, P., Obdržálek, Š., Matas, J., Lourakis, M., and Zabulis, X. (2017). T-LESS: An RGB-D dataset for 6D pose estimation of texture-less objects. *IEEE Winter Conference on Applications of Computer Vision (WACV)*.

IKEA (2017). Place app.

Kendall, A., Grimes, M., and Cipolla, R. (2015). PoseNet: A convolutional network for real-time 6-DOF camera relocalization. *CoRR*, abs/1505.07427.

Krizhevsky, A., Sutskever, I., and Hinton, G. E. (2012). Imagenet classification with deep convolutional neural networks. In *Proceedings of the 25th International Conference on Neural Information Processing Systems - Volume 1*, NIPS'12, pages 1097–1105, USA. Curran Associates Inc.

Le Cun, Y., Jackel, L. D., Boser, B., Denker, J. S., Graf, H. P., Guyon, I., Henderson, D., Howard, R. E., and Hubbard, W. (1990). Handwritten digit recognition: Applications of neural net chips and automatic learning. In Soulié, F. F. and Hérault, J., editors, *Neurocomputing*, pages 303–318, Berlin, Heidelberg. "Springer Berlin Heidelberg.

Li, Y., Wang, G., Ji, X., Xiang, Y., and Fox, D. (2018). DeepIM: Deep iterative matching for 6D pose estimation. *CoRR*, abs/1804.00175.

Lowe, D. G. (1999). Object recognition from local scale-invariant features. In *Proceedings of the Seventh IEEE International Conference on Computer Vision*, volume 2, pages 1150–1157 vol.2.

Microsoft Hololens® (2015-2017). Webpage.

Rad, M. and Lepetit, V. (2017). BB8: A scalable, accurate, robust to partial occlusion method for predicting the 3d poses of challenging objects without using depth. *2017 IEEE International Conference on Computer Vision (ICCV)*, pages 3848–3856.

Ronneberger, O., Fischer, P., and Brox, T. (2015). U-Net: Convolutional networks for biomedical image segmentation. *CoRR*, abs/1505.04597.

Sabour, S., Frosst, N., and Hinton, G. (2017). Dynamic routing between capsules. *CoRR*, abs/1710.09829.

Simonyan, K. and Zisserman, A. (2014). Very deep convolutional networks for large-scale image recognition. *CoRR*, abs/1409.1556.

Szegedy, C., Liu, W., Jia, Y., Sermanet, P., Reed, S., Anguelov, D., Erhan, D., Vanhoucke, V., and Rabinovich, A. (2015). Going deeper with convolutions. In *2015 IEEE Conference on Computer Vision and Pattern Recognition (CVPR)*, pages 1–9.

Xiang, Y., Schmidt, T., Narayanan, V., and Fox, D. (2017). PoseCNN: A convolutional neural network for 6d object pose estimation in cluttered scenes. *CoRR*, abs/1711.00199.

APPENDICES

A T-LESS Viewpoints

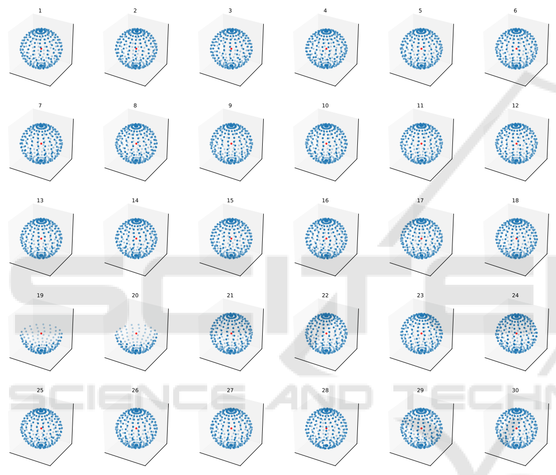

Figure 6: Position where each object is photographed to produce the training data-set. Objects 19 and 20 have a full vertical symmetry, this is why they are only sampled from one side of the sampling sphere. All point-of-view are bounded in the rectangle $(-652.975mm, -652.252mm, -635.481mm)$ to $(651.928mm, 653.682mm, 635.049mm)$.

The Figure 6 presents the positions where the camera shot the picture used to create the training set of the T-LESS dataset.

B Network Architecture

The architecture of the network as well as configuration parameters of every layers are provided in Figure 1. The auxiliary classifiers used during training are both designed following the Figure 2.

C Combined Loss

During training the euclidean loss is applied to all 3 classification branches. It is integrated using the following formula:

$$\begin{aligned} L_{Global}(\widehat{t}, t, \widehat{q}, q) = {} & \lambda_0 \times L_{Aux0}(\widehat{t_{Aux0}}, t, \widehat{q_{Aux0}}, q) \\ & + \lambda_1 \times L_{Aux1}(\widehat{t_{Aux1}}, t, \widehat{q_{Aux1}}, q) \\ & + \lambda_2 \times L_{Top}(\widehat{t_{Top}}, t, \widehat{q_{Top}}, q) \end{aligned} \quad (5)$$

Where L_{Top}, L_{Aux1} and L_{Aux2} are computed using Equation (1) with the same labels but with predictions coming from the different regression branches.

The authors of GoogleNet (Szegedy et al., 2015) suggested to use $\lambda_0 = 0.3$, $\lambda_1 = 0.3$ and $\lambda_2 = 1.0$, this is what is used in PoseNet (Kendall et al., 2015), thus we stick with these values for all our experiments.

D Remarks

Baseline Architecture. Setting $\alpha = 0.01, \beta = 0$ is not equivalent to having a network predicting only translation (7 logits instead of 3), and setting $\alpha = 0, \beta = 1$ is not equivalent to having a network predicting only rotation (7 logits instead of 4): the extra "unused" weights (4 or 3) in the network contribute to the gradient computations and to the regularization terms. Indeed $||W||_2$ is often used to prevent the weights values from taking too large values, where W is the matrix containing all the weights of the network.

Unit Quaternion. The predicted quaternion $\widehat{q}$ is not normalized but the network is optimized with respect to a normalized "label" quaternion $\frac{q}{||q||_2}$, thus it is trained to predict unit length quaternion, but they are no hard constraints for it. This is actually a better idea than to normalize the predicted quaternion $\widehat{q}$ in the loss, as it would not penalize the training if a non-unit quaternion was predicted by the network. Although at test time the predicted quaternion can be normalized for example to later convert it to Euler angles.